Feature-Based Reconstruction of Non-Beam-Like Topology Optimization Design Proposals in Boundary-Representation

Johannes Mayer[1]*, Harald Völkl[1], Sandro Wartzack[1]

[1] Friedrich-Alexander-Universität Erlangen-Nürnberg, Engineering Design, Martensstraße 9, 91058 Erlangen, Germany

* *Corresponding Author:*
Johannes Mayer
Lehrstuhl für Konstruktionstechnik KTmfk
Martensstraße 9
91058 Erlangen
☎ *+49 9131/ 85 23 215*
✉ *mayer@mfk.fau.de*

Abstract

Geometry reconstruction from 3D topology optimization results to Computer Aided Design (CAD) is challenging, especially for automation and non-beam-like geometry. While the optimized model has polygonal format, product development with CAD requires analytical surfaces in Boundary Representation (B-Rep). In this paper, we present two approaches for an automated interpretation of surface-skeletons for CAD-reconstruction. This includes the question, when to convert the skeleton's polygonal to analytical surfaces and how to conceptually incorporate CAD-features. One approach is based on decomposing the input in analytical, the other in polygonal surfaces. Both approaches work with specific skeleton-features and lead to a CAD-model with B-Rep-reconstruction. Exemplary results are presented.

Keywords

Topology Optimization, Computer Aided Design, Geometry Post-Processing, Medial Axis Transform, Skeletonization

 | DOI: https://doi.org/10.35199/dfx2022.21

1. Motivation: Bottleneck of Geometry Postprocessing in the Development of Lightweight Products with Topology Optimization

Topology optimization (TO) has proven to be highly beneficial to produce design proposals for lightweight structures [1-3]. From a given design space, loads and constraints, a design proposal is computed [1]. The design proposal typically is provided as an abstract surface in a triangulated format [4]. It does not have parameters, features, or faces, which could be modified manually by engineers. This way, it is not suited for downstream applications in product development, like structural analysis, parameter variations, variant building or – shortly – design exploration [4]. Practical use of TO requires geometry postprocessing, wherein it still is highly demanding to convert topology optimization design proposals into a CAD-model [1-4]. The design proposal basically represents geometry through a connection of cartesian points forming lines and facets. In polygonal modeling, these constituents can be modified individually up to all together, which is what is used successfully in animation industry. Yet, it does not adequately represent analytical geometry, nor does it correspond to a model, that can be modified efficiently in Computer Aided Design (CAD), which product developers are used to [4]. Technical product development requires analytical surfaces as data-representation. Moreover, to enable CAD-based editing, information on geometric parameters and even features have to be included [4]. While polygonal modelling has other fields of application, analytical surfaces and boundary representation (B-Rep) are predominantly used in the engineering field. Therefore, TO-results have to be converted to B-Rep format. To automate geometry post-processing after topology optimization, research has presented skeletonization based approaches.

2. State of the Art: Skeleton Based Topology Reconstruction from Design Proposals

Geometry postprocessing approaches of this category rely on the abstraction of input geometry through lower-dimensional skeletons. The various skeletonization methods originate in computer graphics, the animation-, game- and CAD-industry. They are suited for computation of middle-lines (curve-skeletons) or middle-surfaces (surface-skeletons). These, in turn, are referenced for the construction of higher-dimensional geometry. Using contraction-based curve-skeletonization, STANGL [5], NANA [6], CUILLIÈRE [7], KRESSLEIN [8] and AMROUNE [9] extrude a defined cross-section along skeleton lines (so called „Sweeping“). This way, parametric 3D-geometry is created, because the cross-section as well as the skeleton itself as guideline, can be parametrically manipulated. Skeleton-lines are manually converted from straight polygonal lines to B-spline-curves in STANGL [5]. Similarly, KRESSLEIN [8] and Amroune [9] perform segmentation and B-spline-conversion, while NANA [6] and CUILLIÈRE [7] normalize in straight line-segments. The software *materialise 3matic* computes skeleton-lines and yields tools for surface-oriented reconstruction [10]. LIU [11] uses curve-skeletonization for smoothing the contour of a 2D shape, before using cubic B-splines. Again related to curve-skeletonization, DENK [12] describes a method with homotopic thinning, where a rasterized voxel model is treated with distance-transform and thinning. In the end, information on cross-section-measures is incorporated within the distance transform. YIN [13] and ALVES [14] use thinning as well. The resulting curve-skeletons are treated under neighborhood-relations, to identify knots. The skeleton is imported to CAD-environment as interconnected straight lines.

In brief, curve-skeleton-methods are partially automated approaches with manual intervention at crucial steps in geometry creation. They are especially suited for beam-like structures. The combination of several cross-sections at crossing points in the topology of the reconstructed volume is a challenge. Moreover, the identification of cross-sections near crossing points is tedious and error-prone. The curve-skeleton near crossing points is prone to deviate from the actual input geometry position. These difficulties are examined by SUBEDI [4], CUILLIÈRE [7], and KRESSLEIN [8]. Contraction-based methods often produce

skeletons outside of the design space volume. Especially non-beam-like structures – small in only one of three dimensions – are difficult to analyze, because line representation can be ambiguous in this case. Figure 1 shows typical difficulties in curve-skeletonization. The example is computed with the contraction-based Mean Curvature Flow algorithm [15]. The skeleton's exact positioning in the design proposal can hardly be anticipated intuitively. On closer inspection, it is asymmetrical and locally out of bounds of the input shape. A reconstruction strategy, which is based on cross-section computation normal to curve-skeleton lines, is hereby hindered. Though skeletons are expected to represent essential shape [16], this relation is restricted in the curve-skeletonization of non-beam-like geometry [4, 7, 8].

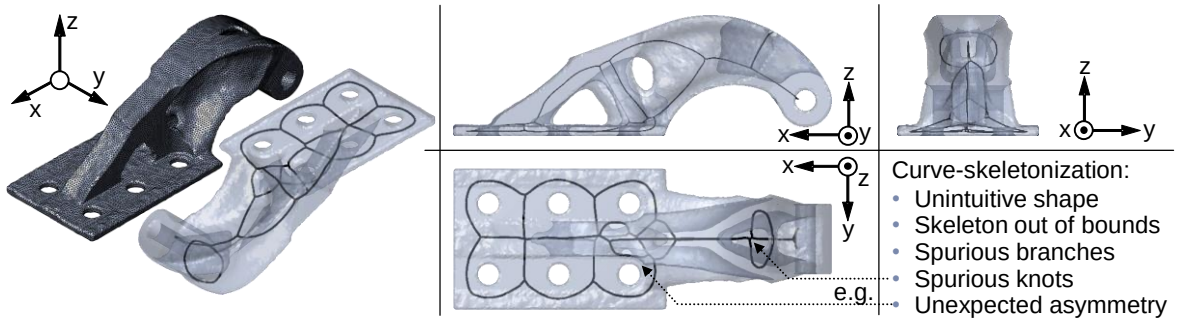

Figure 1: Difficulties in essential abstraction of a non-beam-like geometry with curve skeletonization

Automated geometry reconstruction through curves is restricted. Alternatively, higher dimensional surface-skeleton can be used for geometry reconstruction. Denk [17] uses boundary-curves of surface skeletons for a control grid of subdivision-surfaces. To a limited extent, this enables automatic reconstruction of non-beam-like geometry, but does not incorporate parametrics or CAD-features. In previous work, we also used the boundary of a surface skeleton for the definition of analytical B-spline mid-faces [18].

3. Open Questions in the Automated Interpretation of Voronoi-based computed Surface Skeletons

Automated and feature-based geometry reconstruction is the superior research interest. Curve-skeleton-related strategies are error prone, when applied to non-beam-like geometry. Surface skeletons, on the other hand, have not been the focus of the scientific community up to now. Unlike the 1D curve-skeletons, these abstract 3D geometry with 2D-faces. This seems better suited for non-beam-like geometry in particular. However, the change in dimensionality from 1D (curve-skeleton) to 2D (surface-skeleton) has to be considered, since this has an impact on the skeleton-interpretation: curve-skeletons are interpreted as guidelines for cross-section-extrusion (Figure 2).

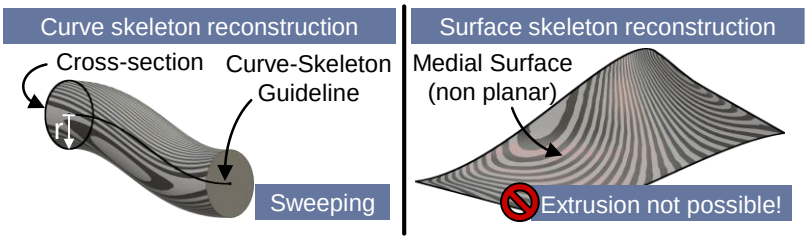

Figure 2: Interpretation of curve skeletons for geometry reconstruction through sweeping operation with cross section and guideline (left) and difficulty of interpretation of surface-skeleton (right).

It stands to reason, that every curve-skeleton can easily be segmented by its cross-points. That way, reconstruction can be implemented as a parametric feature. Analytical B-Rep-faces are already computed within this feature. The result is exportable in standardized data exchange format.

Surface skeletons require a less trivial procedure. Although simple face-extrusion seems to be obvious, this usually is not possible, because faces are not flat or planar [18]. Also, there are no strictly separated faces or closed surface-segments in the first place [19]. Instead, it is a matter of triangulated, small scale facets. These are hardly segmentable. Consequently, the following questions are addressed: How should surface skeletons be automatically interpreted? How to implement parametrics and features? These research questions are addressed in the following section 4.

4. Methods for Geometry Reconstruction with Voronoi-based Surface Skeletons

4.1. Overview

The three-step process is presented in Figure 3. The input always is TO's design proposal in any triangulated data format. First, the geometry is abstracted through skeletonization. As the immediate surface skeleton is not sufficient for reconstruction, the skeleton-data has to be processed to an overall decomposition-structure. This means the entirety of all information necessary for reconstruction. This includes skeletonization-data, their editing, geometry data on ideal geometry elements and, if necessary, manual adjustements. The third step is a parametric reconstruction, where in the end parametric and feature-based B-Rep geometry is provided. Though substeps range from manual to fully automated, the prevailing number of substeps are automated. In detail, this is explained in the following sections.

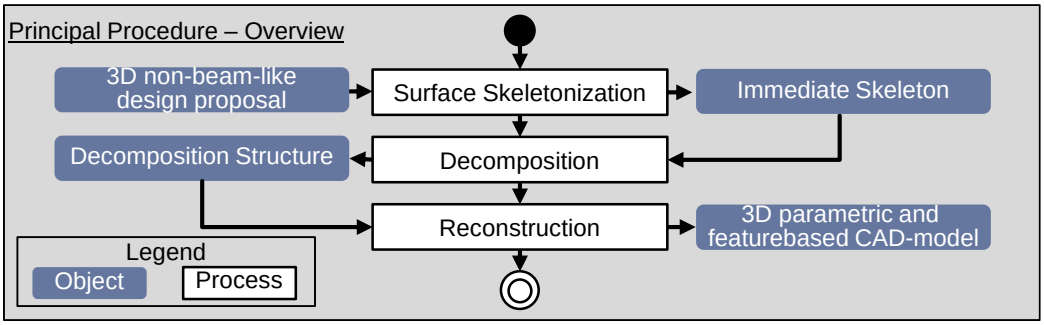

Figure 3: Procedure in our skeleton-based reconstruction of 3D non-beam-like design proposals

4.2. Skeletonization and Decomposition with the Medial Axis Transform

Surface-skeletons originated as mathematical shape descriptor [20]. Contrary to the common Boundary Representation, these describe a shape alternatively by the set of centers of maximally inscribed balls [16, 20, 21]. The infinite set of the union of balls is called medial axis transform (MAT) and can be considered information-equivalent and dual to B-Rep [16, 20]. Because the exact computation of the MAT is difficult, oftentimes a simplified, approximate version with a finite set of medial balls is computed [21]. We use a Voronoi-diagram for MAT-computation. The vertices of a 3D Voronoi diagram are fundamental for the medial axis because they are equally distanced from at least two nearest input points. Though this property suits the definition of medial balls, the Voronoi vertices in general are not sufficient for medial axis computation. First, they lie both inside and outside of the input shape. Second, amongst the in- and outliers respectively a subset of Voronoi-vertices has to be computed, which are the so-called poles [21]. The outer poles build the outer medial axis, while the inner poles build the desired inner medial axis skeleton, shortly referred to as medial axis onwards.

Preliminaries: For computation, the requirement of sufficiently dense sample points (input points) has to be fulfilled. In our approach, this is assumed to always be the case, since the mesh of the design proposal can be subdivided to arbitrary fine structure. Unlike the method of AMENTA [21], that processes point clouds, our input doesn't need to be C_2-smooth for a determination of interior and exterior. Instead, we can fall back on input surface-normals. The input triangulation is not necessarily fulfilling any requirements on edge intersections and is non-manifold in most cases. So, as a first step, it is isotropically remeshed into a manifold mesh. Remeshing guarantees equally spaced vertices, which later effects the medial axis to also have equally spaced skeleton-vertices. The design proposal as raw output of the TO typically has lots of salient characteristics. The medial axis transform represents every salient element from the initial shape [21]. For this reason, the design proposal's triangulation is firstly smoothed through averaging each node's position by its direct neighbors. This is an approximated Laplacian smoothing. It is repeated in a heuristic number of iterations. The smoothing only aims for cancelling out the rough salient elements and keeps the basic information of material distribution untouched.

Skeletonization: Then, the medial axis skeleton is computed. Resulting from the MAT-computation is a triangulated surface, whose node-connectivity originates from the connectivity of respective input points. The medial axis skeleton's mesh quality is poor, with overlaying edges, redundant nodes and non-manifold geometry. From an interpretation point of view, the design proposal's geometry is depicted qualitatively, not explicitly. For example, junction-elements are not represented by a single edge in the skeleton, but by several, jagged edge-segments. Also, the boundary cannot be identified without further action. Informally put, the medial axis computation could be imagined with vacuum-packing a volume. The medial axis locates where opposing surfaces meet. This results in several surface-segments stacked into each other, which complicates the geometric data structure. In addition, the medial axis represents even the slightest unsteadiness in the geometry as large slivers in the skeletal form. Due to these reasons, the reconstruction of the desired CAD-model can't be based on the skeleton itself. It takes processing and additional data for feasible geometry reconstruction, if this step has to be performed in an automated algorithm. We call this consumption of data the decomposition structure.

Decomposition: Several steps after skeleton computation are performed. To clean the MAT from unnecessary elements, we perform a further smoothing in case that the first smoothing has not yet prevented the medial axis to show salient characteristics. The smoothing works according to the same principle explained before. This time, it is applied on the medial axis. Also, very closely neighbored verts are merged in postponed processing. Facets, radii and vectors are adapted. The postprocessing simplificates data without information loss.

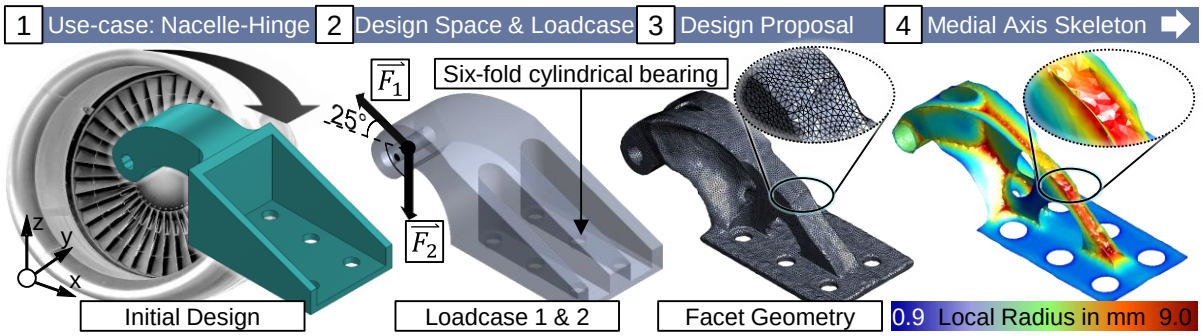

Figure 4: First steps in our medial axis based geometry reconstruction with the use-case of a nacelle-hinge. Shown are the initial design (1.) from [22], the loadcases (2), the design proposal (3.) and the medial axis skeleton coloured according to cross-section-thickness (4.).

As demonstrator throughout this paper the turbine nacelle hinge from TOMLIN and MEYER [22] is chosen for its non-beam-like geometry and its practical background. In an aero engine, the part is used to attach a large side door to the main structure. TOMLIN and MEYER [22] describe an optimization process and conventionally manual re-design with iterative design cycles.

Led by this example, the capabilites of the proposed procedure are examined. Figure 4 shows the initial design, the topology optimization loadcases, TO's design proposal as well as the medial axis skeleton computed with our algorithm. In TO structures, oftentimes some part-areas are excluded from optimization. Functional aspects like the connection to adjacent components for instance, may require material to be placed at respective areas either way. Those are not participating in the TO. Therefore, the non-design domain is found again identically in the design proposal. This is a special property, because otherwise, the design proposal's surface shows salient characteristics. This property is exploited by automatically identifiying ideal geometry in the design proposal. This is done through comparison between design proposal's abstract surface and the design space. Ideal geometry elements are automatically extracted as analytical B-Rep-elements to the decomposition-structure. Briefly, material unaffected by TO is directly turned to B-Rep and kept for the reconstruction step.

4.3. Analytical Decomposition and Reconstruction

Results of our MAT-computation include the radii of the medial balls. Those are highly interesting for geometry reconstruction, because they are direct geometric data. A medial radius can be equally interpreted as cross-section-thickness. Further results of the MAT-computation include the specific input points, which lie on the medial ball around a specific node of the medial axis. Those are the so called feature points. Similarly, the vectors from the medial axis to those points are the feature-vectors. Vice versa, the connection from a specific input point to their respective closest medial axis point is computed, which is not necessarily identical to the list of feature-points and -vectors.

Boundary-facets can be automatically identified by filtering facets of low area (Fig. 5, see 5a). Next, details like the leftover boundary of boreholes are deleted manually. This simplifies the boundary facets (Fig. 5, see 6a). Then, every line of the boundary-facets is automatically offsetted to a cylindrical mesh-structure (Fig. 5, see 7a). This beam-like structure is skeletonized with curve-skeletonization, in order to yield a polyline representing the surface-skeleton's boundary. This basically is a workaround starting with the unordered boundary-facets and with the goal to identify the medial axis skeleton's boundary as a curve of simple connectivity. The polyline is then turned into a B-spline-curve (Fig. 5, see 8a) [18].

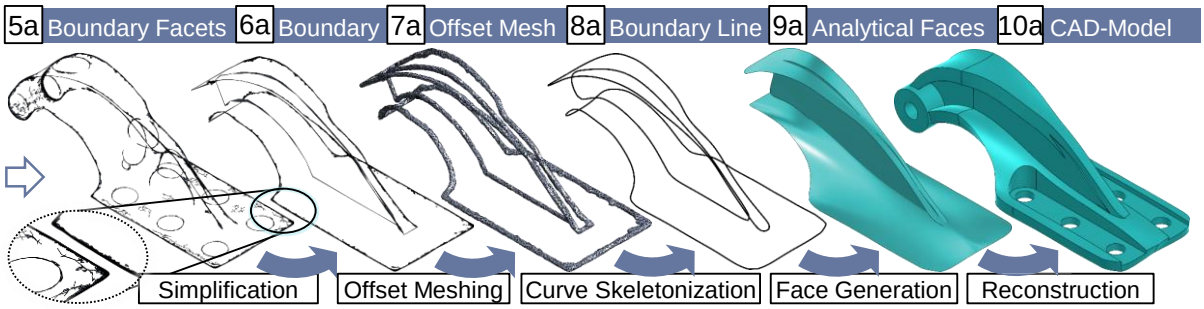

Figure 5: Decomposition and reconstruction-process through identification of boundary-facets and simplification, offset meshing, deriving boundary-lines, computation of analytical surfaces and the final CAD-model.

In order to automate the reconstruction process, the algorithm identifies which loops in the boundary-lines represent a single face. This is a sub-process of its own. In Figure 5, this results in three closed loop-segments, for each of which a B-Spline-face is created (Fig. 5, see 9a).

Reconstruction: The 3D positions of the medial axis vertices can be used as constraints for the generated faces. For this, automatically assigning them to a face is necessary. The respective face then is re-calculated according to its subset of medial axis verts. This can lead to undesired distortion of the B-Spline-face. In this case, the faces' adaption to specific subsets of medial axis verts is waived. Since extrusion is not possible either way, and the geometric information in the radii of the MAT should be considered, a special dilatation-feature is developed. If consideration of medial axis verts is waived, this corresponds to a "thickening"-feature in CAD. Otherwise, each face is copied twice and offsetted along the mean feature-vector of the faces medial axis vertices. Then the offsetted faces are adapted to the previously mentioned feature-points. This way, the B-Rep surface of the reconstructed model is set up. The last steps include consideration of previously mentioned ideal geometry elements and the manifold combination of the generated faces to a solid body.

4.4. Polygonal Decomposition

The preceding strategy, which focuses on B-Rep-structure from the beginning, is confronted by tedious issues through the attempted consideration of medial axis vertices in the generation of the B-Rep surface. The susceptibility to errors motivates the development for an alternative decomposition-structure that is easier to manage. Instead of finding the boundary-line (sec. 4.3), this strategy is built on polygonal modelling in adaption from graphic and animation industry. Accordingly, the medial axis skeleton (Fig. 4, see 4) is manually reconstructed with corse quad-mesh-elements (Fig. 6, see 5b). This is a known workstep in the graphics community under the term "retopology".

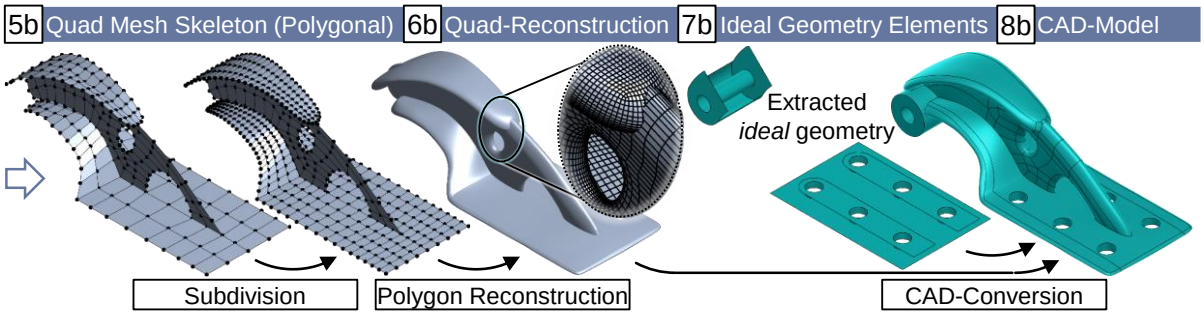

Figure 6: Decomposition and reconstruction process through skeleton remodelling in a polygonal mesh, subdivision, dilatation to a volume body, extension by ideal geometry elements and the final CAD-model.

Reconstruction: Through retopology, the skeleton is simplified. This is a full quad-mesh, free of intersections, and low in storage requirement due to the small number of vertices. If more detailed distribution of vertices is necessary, a subdivision can automatically be performed to any degree (Fig. 6, see 5b). Alike the analytical reconstruction process, the geometric information of cross-section-thickness within the medial axis radii is used. Thus, since the skeleton structure has changed drastically from non-manifold triangulated facets to quads, the radii are mapped to the new data structure. This is done automatically with nearest neighbor seach between mesh nodes from previous and current set. The radii are superimposed according to the nearest neighbor found. Based on the radii as thickness information and the quad-skeleton as location, the quad-mesh is dilated (Fig. 6, see 6b). As a next step, the quad-mesh is converted to analytical surfaces in CAD-environment. The final CAD-model is derived through extension by boolean operations with the previously extracted ideal geometry elements (Fig. 6, see 7b/ 8b).

5. Results and Discussion of B-Rep- and polygonal decomposition

Immediate results are the CAD-models provided by the applied approaches as shown in section 4.3 and 4.4. In the application for the nacelle hinge, strategy 1 requires manual interventions in the decomposition. Some superfluous facets have to be removed after the boundary recognition in places around the boreholes, while they have to be added in the place of the central bar (Fig. 5). There, smoothing did not lead to a shrinking of facets, which is why they are not filtered during boundary-recognition. In case of this demonstrator, the automated B-spline-face-generation from the boundary gets distorted as soon as medial axis vertices are considered as constraints. Therefore, the skeleton is unconstrained and the faces in the reconstruction are generally offsetted instead of using the feature-point-constraint. In order to not exceed design space, manual design intervention is necessary for removing the area above the bore holes (Fig. 5). Further in the reconstruction step, the proposed ideal geometry elements have to be considered. They are easily incorporated as they are provided in standard data format for analytical surfaces. The final CAD-model has B-Rep structure. Though substantial automation is the goal in strategy 1, therefore, more manual intervention is necessary than in strategy 2.

Strategy 2 requires remodelling of the skeleton in a quad-mesh. This is the main difference to strategy 1, because at this point, the skeletal representation is still of polygonal format. After the automatic dilatation in consideration of the MAT and reconstruction, the ideal geometry is incorporated by simple boolean operations. This leads to a short amount of time from design proposal to CAD-model. Directly compared to strategy 1, the medial axis radii are used as reference for the reconstruction feature. The process is faster and less error prone.

Further comparison of the results is based on structural characteristics. The reconstruction geometry is examined together with the initial design of the nacelle hinge and the design proposal. A static structural finite element analysis is carried out with the two loadcases from the optimization. The loading is identical for all models and orients to the condition by TOMLIN and MEYER [22]. Although there are no absolute values for the loads by TOMLIN and MEYER [22], comparison is possible since the analysis stays in the elastic area. We choose 10 kN for each force applied. Material characteristics are isotropic and identical for all models, as they were in the preceding TO. The applied constraints are cylindrical clamping at the six boreholes.

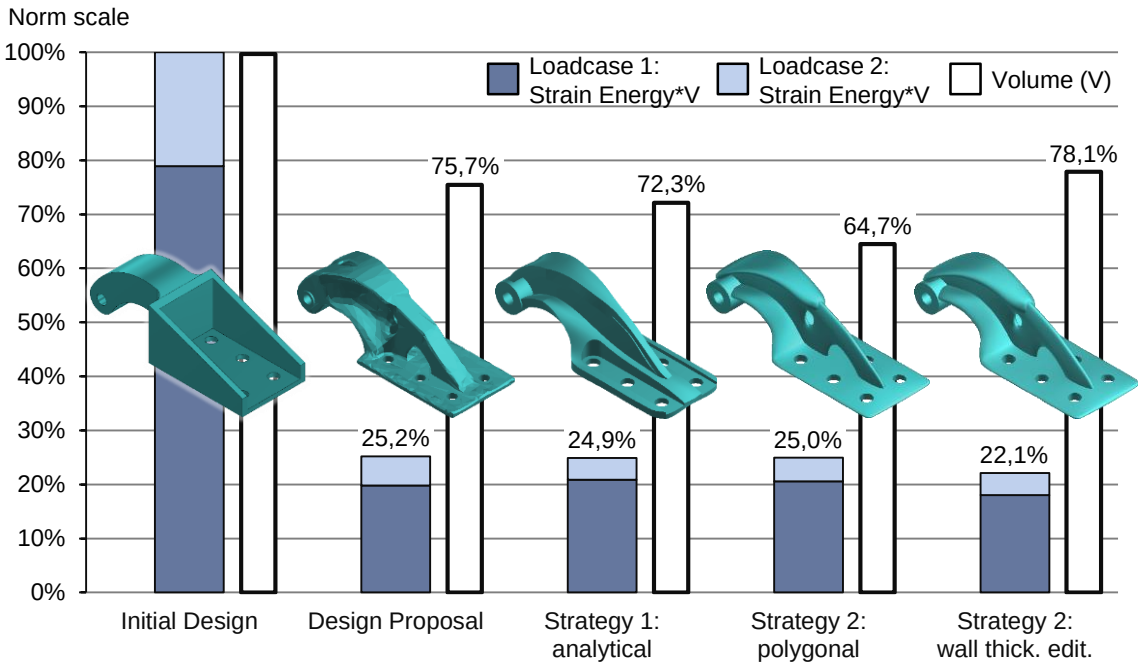

Figure 7: Strain energy and volume of several designs for comparison regarding stiffness and mass

The strain energy for the respective loadcases is used as stiffness measure. Lower values mean better stiffness. Deviation in the volume between the models is considered in multiplication of strain energy and volume. Volume itself is shown as well. The scale is unified to the results of the initial design, to put performance into context. Also, the design proposal's results are added for further relation.

All optimized models have clearly less strain energy and mass than the initial design. For the second loadcase, strategy 1 shows slightly better stiffness compared to the design proposal. This may originate in slight design space exceedance and the free interpretation of the design proposal in the area of the pin-bolt. While the design proposal splits into a branched structure, the reconstructed models remain with the I-profile throughout. Overall, the reconstructed versions (strategy 1 and 2) are at a very similar level with the design proposal. A valuable benefit is shown by the possibility of exceedingly quick editing in strategy 2. The overall wall thickness was increased by raising every medial axis radius by 25 %. Of course, this changes volume-settings and design space constraining compared to the design proposal, so that the TO-result is not to be doubted. The automatically adapted result has the best stiffness in relation to the mass in the comparison.

6. Summary

Geometry in the context of skeleton-based reconstruction can be divided into beam-like and non-beam-like structures. Aside academic demonstrators, real life geometry components often have non-beam-like (sub-)sections. The generality and variety in geometry causes a challenge for automated reconstruction methods. Fully automated geometry reconstruction for general TO results remains a true challenge. Both of our two presented approaches do not reach to 100 % automation. Approach 1 builds upon the identification of the surface-skeleton's boundary-curves and the calculation of B-Spline-faces from them. It aims for analytical face-representation from the beginning onwards. Approach 2 builds upon the quad-mesh-simplification of the surface skeleton and dilatation to volume geometry under consideration of medial axis geometry information. Herein, the analytical B-Rep-Structure is created subsequently. Our approaches aim for practical product development. They focus on demanding non-beam-like geometry. The results for the nacelle hinge show stiffness properties at a similar level with the TO design proposal. Also, the quick and easy design exploration is allowed by approach 2. It is a considered strength, that the approaches are based on the design proposal, but not tied to it. This helps with guided interpretation, but also opens up the freedom for design exploration. In combination with the possibility of feature- and parameter editing reconstructed models, can even be improved. The approaches finally yield an analytical CAD-model. This way, geometry postprocessing can be usefully applied in product development. TOMLIN and MEYER [22] explain, that slightly different hinges with slightly different geometry and loadcase are required per aero engine. In just such cases an automated reconstruction method helps integrating TO in the process, accelerates and ensures lightweight product design.

Acknowledgement

The presented research work is funded by the Deutsche Forschungsgemeinschaft (DFG, German Research Foundation) – WA 2913/36-1 with the title „TopoRestruct – Rückführung fertigungs-, beanspruchungs- und funktionsgerechter Konstruktionsgeometrie aus Ergebnissen der Topologieoptimierung in den Produktentwicklungsprozess". The authors thank the German Research Foundation for the financial support.

References

[1] Bendsøe, M. P.; Sigmund, O.: Topology Optimization: Theory, Methods and Applications. Berlin, Heidelberg: Springer, 2004.

[2] Schumacher, A.: Optimierung mechanischer Strukturen - Grundlagen und industrielle Anwendungen. Berlin, Heidelberg: Springer, 2013.

[3] Harzheim, L.: Strukturoptimierung: Grundlagen und Anwendungen. Europa-Lehrmittel, 2014.

[4] Subedi, S.; Verma C. S.; Suresh K.: A review of methods for the geometric post-processing of topology optimized models. J. Comput. Inf. Sci. Eng. Bd. 20 (2020) Nr. 6.

[5] Stangl, T.; Wartzack, S.: Feature based interpretation and reconstruction of structural topology optimization results. In: Weber, C.; Husung, S.; Cascini, G.; Cantamessa, M.; Marjanovic, D.; Graziosi, S. (Hrsg.): Proceedings of the 20th International Conference on Engineering Design (ICED15). Milan/ Italy. 2015.

[6] Nana, A.; Cuillière, J.-C.; François, V.: Automatic reconstruction of beam structures from 3D. Computers & Structures. Bd. 189 (2017), S. 62–82.

[7] Cuillière, J.-C.; François, V.; Nana, A.: Automatic construction of structural CAD models from 3D topology optimization. Computer Aided Design and Applications. Bd. 15 (2017) Nr. 1, S. 107–121.

[8] Kresslein J. et al.: Automated cross-sectional shape recovery of 3D branching structures from point cloud. Journal of Computational Design and Engineering. Bd. 5 (2018), S. 368–378.

[9] Amroune, A.; Cuillière, J.-C.; François, V.: Automated Lofting-Based Reconstruction of CAD Models from 3D Topology Optimization Results. In: Computer-Aided Design. Bd. 145 (2022) Nr. 1, doi 10.1016/j.cad.2021.103183.

[10] Blanc, C.: 3-matic STL 9.0. Von der Topologieoptimierung zum gedruckten Bauteil, Materialise beschreitet neue Wege, in 11. Coachulting Forum, 2015.

[11] Liu, S. et al.: A realization method for transforming a topology optimization design into additive manufacturing structures. Engineering. Bd. 4 (2018), S. 277–285.

[12] Denk, M., Rother, K.; Paetzold K.: Fully Automated Subdivision Surface Parametrization for Topology Optimized Structures and Frame Structures using Euclidean Distance Transformation and Homotopic Thinning. In: Pfingstl, S.; Horoschenkoff, A.; Höfer, P.; Zimmermann, M. (Hrsg.): Proceedings of the Munich Symposium on Lightweight Design 2020. Berlin, Heidelberg: Springer, 2021.

[13] Yin, G.; Xiao, X.; Cirak, F.: Topologically robust CAD model generation for structural optimisation. Computer Methods in Applied Mechanics and Engineering. Bd. 369 (2020).

[14] Alves, C. G.; Siefkes T.: Automatische Erstellung von Drahtgittermodellen aus Topologieoptimierungen.In: Stuttgarter Symposium für Produktentwicklung SSP 2021. Stuttgart/ Deutschland, 2021.

[15] Tagliasacchi, A. et al.: Mean Curvature Skeletons. Eurographics Symposium on Geometry Processing 2012. Bd. 31 (2012) Nr. 5, S. 1735–1744.

[16] Tagliasacchi, A. et al.: 3D Skeletons: A State-of-the-Art Report. In: Madeira, J.; Patow, G.; Romão, T. (Hrsg.): Computer Graphics Forum. Bd. 35 (2016) Nr. 2.

[17] Denk, M.; Rother, K.; Paetzold, K.: Subdivision Surface mid-surface reconstruction of topology optimization results and thin-walled shapes using surface skeletons. In: International Conference on Engineering Design, ICED21, Gothenburg/ Sweden, 2021.

[18] Mayer, J.; Wartzack, S.: A concept towards automated reconstruction of topology optimized structures using medial axis skeletons. In: Pfingstl, S.; Horoschenkoff, A.; Höfer, P.; Zimmermann, M. (Hrsg.): Proceedings of the Munich Symposium on Lightweight Design 2020. Berlin, Heidelberg: Springer, 2021. ISBN 978-3-662-63142-3.

[19] Mayer, J.; Wartzack, S.: Investigation of surface skeletonization methods for reconstruction of topology optimized structures. In: Krause, D.; Paetzold, K.; Wartzack, S. (Hrsg.): Proceedings of the 31st Symposium Design for X (DFX2020). Design Society, 2020, S. 111–120.

[20] Blum, H.: A Transformation for Extracting New Descriptors of Shape. In: Wathen-Dunn, W.(Hrsg.): Models for the Perception of Speech and Visual Form. Cambridge: MIT Press, 1967. S. 362–380.

[21] Amenta, N. et al.: The Power Crust. In: Proceedings of the 6th ACM Symposium on Solid Modeling and Applications. New York, NY, USA: ACM, 2001, S. 249–266.

[22] Tomlin, M.; Meyer, J.: Topology Optimization of an Additive Layer Manufactured (ALM) Aerospace Part. The 7th Altair CAE Technology Conference, Gaydon, 2011.